Melt Rheology of High L-Content Poly(lactic acid)

Liviu-Iulian Palade,* Hans J. Lehermeier, and John R. Dorgan*

Department of Chemical Engineering, Colorado School of Mines, Golden, Colorado 80401-1887

Received July 6, 2000; Revised Manuscript Received November 17, 2000

ABSTRACT: The melt rheology of linear poly(lactic acid)s (PLA) characterized by a high content of the L-form of the monomer is comprehensively investigated. Measurements of dynamic, steady, and transient shear viscosities are presented. Extensional data on PLA are presented for the first time and show a strong strain hardening behavior. The Cox−Merz relationship is obeyed over a particularly wide range (roughly 3 decades of shear rate). Results for high molecular weight samples suggest that the plateau modulus is approximately 5×10^5 Pa. In addition, the zero shear viscosity, η_0, for these materials is found to roughly scale with the expected 3.4 power vs molecular weight. The transient shear results are satisfactorily predicted using a truncated form of the K−BKZ constitutive equation and a set of Maxwell modes (G_k, λ_k) derived from the dynamic spectra. However, to capture the observed extensional hardening, an additional long time relaxation mode must be added to the spectrum. Time sweep measurements demonstrate that the melt stability of the polymer precludes long time measurements. Chemical changes manifest themselves in a lack of adherence to the principle of time−temperature superposition. It is shown that stabilization of poly(lactic acid) using tris(nonylphenyl)phosphite is possible and leads to a material that is thermorheologically simple within the experimentally assessable rates of deformation.

Introduction

Pressing environmental and economic concerns dictate the need to develop new synthetic macromolecules based on renewable resources. The vast majority of existing materials are based on nonrenewable fossil resources, which will eventually be extinguished. In addition, both the manufacture of synthetic polymers and their disposal by incineration produces CO_2 and contributes to global warming. Many widely used polymer materials, notably polystyrene and poly(vinyl chloride), are made from noxious or toxic monomers. Consequently, there is a need for the development of "green" materials that would be based on renewable resources, would not involve the use of toxic or noxious components in their manufacture, and could allow composting to naturally occurring degradation products or could be recycled easily. For this reason, poly(lactic acid) (PLA) polymers are of increasing commercial interest since they are derived from a renewable agricultural resource (corn), sequester significant quantities of carbon dioxide relative to petrochemical-based materials, provide significant energy savings, and easily degrade by simple hydrolysis. Further details of the economic and environmental benefits of PLA are available elsewhere.[1,2]

Clearly, for PLA to be adopted on a wide scale for use as a conventional thermoplastic, its rheological properties in the melt must be understood in order to facilitate effective processing. Despite this need, relatively few studies have appeared in the open literature. Work on mechanical properties in the solid state has appeared,[3,4] and on the basis of modulus measurements of PLA, Grijpma et al. report a value for the plateau modulus of $G^0_N = 5 \times 10^5$ Pa.[4] However, little additional melt rheological data are available. One noteworthy study is that of Witzke and co-workers that summarizes many of the physical properties of PLA and provides some rheological data on linear architectures.[5] Cooper-White and Mackay also reported on the melt rheological properties of poly(L-lactic acid) and provided a value for the plateau modulus of $G^0_N = 5.5 \times 10^5$ Pa; they report scaling of the zero shear viscosity, η_0, with molecular weight to the 4.0 power.[6] However, only four samples were investigated. Dorgan et al. performed a study on linear and star architectures and discussed the effects of long chain branching in these materials.[7] Ramkumar and Bhattacharya performed a study on three different families of degradable polyesters including PLA; limited melt rheology data for two samples varying in L:D content are reported.[8]

This paper presents a more comprehensive study of the melt rheological properties of high L-content PLA than has been published previously. Extensional viscosity measurements are presented for the first time. Measurements of dynamic, steady, and transient shear are presented. The effects of degradation and stabilization of PLA on rheological behavior are also discussed. Data from different sources are collected and presented to show that the scaling of the zero shear viscosity with molecular weight does not vary significantly from the usual 3.4 power. Modeling of the results is also undertaken using a truncated K−BKZ constitutive equation with a time−strain factorized relaxation function. The time dependence is represented as a series of elementary Maxwell modes (G_k, λ_k) derived from dynamic measurements. It is shown that the observed strain hardening under extension requires the addition of an additional long time relaxation mode not observed in the dynamic measurements.

Experimental Section

Because of the chiral nature of lactic acid, the stereochemistry of PLAs is complex. Figure 1 shows the L- and D-enantiomers of lactic acid along with two possible dimer rings. These lactide ring structures are formed via reactive distillation of an aqueous lactic acid solution. Since the L-lactic acid is available from fermentation, the LL-lactide is of greatest industrial interest. However, some racemization occurs during the distillation to produce the LD-lactide (the meso structure). Control of the ratio of the L- to D-content is an important

* Corresponding authors. E-mail: LPalade@mines.edu; jdorgan@mines.edu.

10.1021/ma001173b CCC: $20.00
Published on Web 01/26/2001

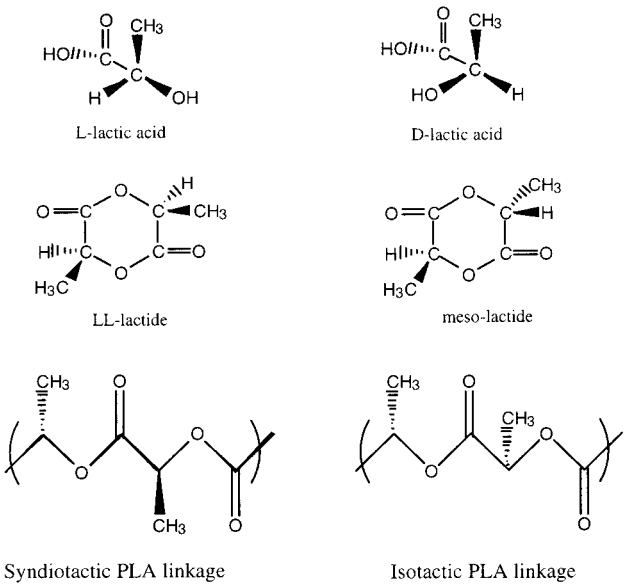

Figure 1. Chemical structure of PLA and its constituent monomers.

molecular feature of PLAs. Polymerization of the pure LL-lactide or the DD-lactide produces completely syndiotactic materials. Mixing of these monomeric forms produces a polymer in which the strict stereoregularity is disrupted.

The PLA samples used in this study were provided by Cargill-Dow Polymers and were melt synthesized using stannous octoate as a catalyst. In this report, results are presented for PLAs having a large L-content (96−100%). Materials were made available as granular pellets. Special care was used in handling all samples to exclude moisture due to the possibility of hydrolytic degradation.

PLA pellets were held in a vacuum oven at 40 ± 1 °C for at least 48 h prior to manipulation. For some tests, chemical stabilization of the PLA samples was accomplished by adding tris(nonylphenyl)phosphite (TNPP). This was done by mixing PLA pellets with different amounts of TNPP in a Haake Rheodyne 5000 mixing bowl at 180 ± 1 °C until a constant torque was observed (i.e., for about 12 min). The samples were then immediately compression molded at 180 °C to get disks having a diameter of 25 mm and a thickness of approximately 2.5 mm. These disks were held in a vacuum oven at 40 ± 1 °C for at least 48 h prior to testing. For extensional testing, bars of 60 mm × 8 mm × 1.5 mm were compression molded in the same fashion.

Shear rheometry has been carried out on a Rheometrics RMS-605 mechanical spectrometer using standard 25 mm parallel plates and 0.1 rad cone and plate configurations. A special pressure canister containing molecular sieves and drierite was installed in the inlet air line to the oven in order to exclude moisture and minimize hydrolytic degradation during testing. All dynamic measurements were carried out within the linear response domain (i.e., where the relaxation moduli are independent of strain amplitude).

Capillary measurements were performed in a Kayeness LCR5000 capillary rheometer. A capillary die having an L/D of 30 was employed, and the Rabinowitsch correction was applied to the data.

Elongational measurements were performed on a Rheometrics RME instrument. Tests were performed at a temperature of 180 °C and at an elongation rate of $\dot{\epsilon} = 0.1\ s^{-1}$ using rectangular shaped samples. These data were corrected according to the results of a round-robin evaluation of the performance and accuracy of this instrument.[9] That is, video recordings were used to measure the true elongational rate according to the protocol developed under the round robin.

Molecular weight and its distribution were measured by gel permeation chromatography (GPC) coupled to light scattering. These experiments were performed at 35 °C in chromatography grade tetrahydrofuran (THF) using 3XPLgel 10 μm columns at a 1 mL/min flow rate. For the GPC calibration a series of 12 narrow molecular weight polystyrene standards (molecular weights between 1925 and 6.3×10^6 g/mol, American Polymer Standards Corp.) were used. Molecular weights were measured for samples before and after being recovered from testing.

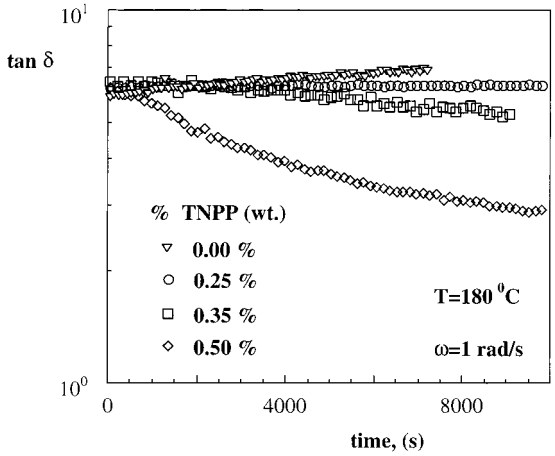

Figure 2. Tan (δ) vs time for a 98:02 PLA containing different concentrations of TNPP.

Results and Discussion

Figure 2 shows time sweep results within the linear viscoelastic regime for a PLA having a composition of 98:02 in terms of the L:D ratio. The measured value for $\tan(\delta) = G''/G'$ as a function of time is presented for materials treated with differing amounts of TNPP. It is clear from the figure that an untreated PLA (0.0 wt % TNPP) exhibits an increasing $\tan(\delta)$ as a function of time. The complete data show that both the storage modulus G' and the loss modulus G'' decrease over time; however, G' decreases more quickly than G'', thus leading to this increase in $\tan(\delta)$. For the highest TNPP concentration shown (0.5 wt %), $\tan(\delta)$ strongly decreases as time progresses. The complete data show that both G' and G'' actually increase during this period of time; however, G' increases more quickly than G'', leading to a decrease in $\tan(\delta)$. A concentration of 0.35 wt % produces the same result but to a much lesser extent. At the concentration of 0.25 wt % TNPP it is seen that the $\tan(\delta)$ values remain constant. The complete data show that both G' and G'' remain constant as well. It is concluded that by adding 0.25 wt % of TNPP to PLA a stable viscoelastic response can be obtained for more than 2 h and 45 min at 180 °C.

Organophosphites are known to stabilize polyesters through participation in complex reaction sequences that effectively suppress hydrolytic degradation and ester exchange reactions.[10] These chemical reactions can prevent chain scission reactions and other thermal degradation. Degradative reactions can cause decreases in molecular weight, thus dramatically affecting the rheological behavior. Table 1 lists the weight-average, the number-average, and the $(z + 1)$-average molecular weights and for each of the samples represented in Figure 2. Before and after headings refer to the rheological testing. Because of changes taking place in the Haake mixer during the addition of TNPP, the samples do not start at exactly the same molecular weight. In addition, it can be clearly seen that the weight-average

Table 1. Molecular Weights for 98:02 PLA Samples Stabilized with TNPP before and after the Measurements of Figure 7

TNPP (wt %)	M_w (g/mol) × 10^3		M_n (g/mol) × 10^3		M_{z+1} (g/mol) × 10^3	
	before	after	before	after	before	after
0.00	120		52		336	
0.25	115	115	55	50	1345	1330
0.35	115	120	55	55	1305	1360
0.50	105	110	50	50	1260	1305

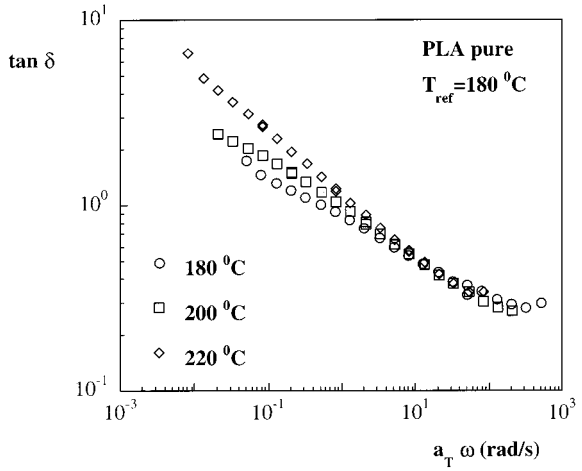

Figure 3. Attempted superposition of tan(δ) vs reduced frequency $a_T\omega$ for a very high molecular weight (750K g/mol) PLA having a 100:0 ratio in L:D content.

molecular weights increase in the cases corresponding to 0.35% or 0.50% TNPP addition due to chain extension. That is, alcohol and carbonyl groups react more readily in the presence of organophosphites. However, the judicious choice of 0.25% TNPP provides the appropriate stabilization to keep the weight-averaged molecular weight approximately constant; this is naturally manifested in the constant material properties measured. These results also confirm the importance of the weight-averaged rather than the number-averaged molecular weight in dictating mechanical response. It is worth noting that PLA must be processed at temperatures around or above 180 °C in order to be in the melt state (T_m is around 170 °C). Consequently, unstabilized PLA materials are expected to lose molecular weight during processing operations characterized by long residence times.

The rheological consequences of degradation in unstabilized PLA are illustrated in Figure 3. This graph shows an attempt to built a master curve of tan(δ) vs the reduced frequency $a_T\omega$ using dynamic shear data obtained from 500 rad/s down to 0.05 rad/s for three different temperatures (180, 200, and 220 °C). Testing was performed by starting at the highest frequency (500 rad/s) and stepping to the lowest one (0.05 rad/s). Samples experiencing a short thermal history (corresponding to high frequencies in these tests) produce a satisfactory overlapping of the curves for almost two frequency decades. However, longer thermal exposures produce significant departures from time temperature superposition due to the ongoing chemical degradation. Moreover, the highest temperature (220 °C) shows the strongest deviation from superposition. Such behavior is consistent with the observation of faster chemical degradation at higher temperatures.

Figure 4 shows the dynamic moduli G' and G'' at 180 °C for the high-frequency, short testing time, region.

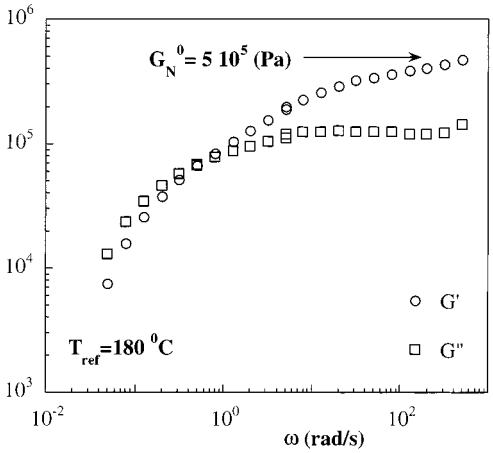

Figure 4. High-frequency values of the dynamic moduli G' and G'' for a very high molecular weight (750K g/mol) PLA having a 100:0 ratio in L:D content. Degradation is negligible during the course of this short experiment and provides a value of the plateau modulus equal to 5×10^5 Pa.

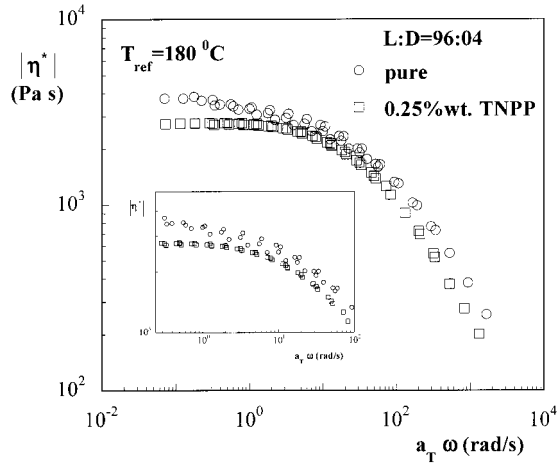

Figure 5. Superposition of $|\eta^*|$ vs reduced frequency $a_T\omega$ at a reference temperature of 180 °C for a high molecular weight (M_w = 110K g/mol) PLA having a 96:04 ratio in L:D content. Both pure PLA (unstabilized) and PLA stabilized with TNPP are shown. The inset shows the improvement in superposition achieved upon stabilization.

Because of the limited thermal exposure, the high-frequency region is unaffected by degradation and can be used to obtain an estimation of the plateau modulus. The high molecular weight of the sample (750K g/mol) makes the plateau region experimentally assessable; however, the polydispersity of the sample ($p \approx 2$) produces some curvature in the plateau region. The estimated value of $G^0_N = 5 \times 10^5$ Pa is in good agreement with previous values reported by Dorgan et al. ($G^0_N = 5 \times 10^5$ Pa),[7] by Cooper-White and Mackay ($G^0_N = 5.5 \times 10^5$ Pa),[6] and by Grijpma et al. ($G^0_N = 5 \times 10^5$ Pa).[4] However, these consensus values are all higher than the value reported by Ramkumar and Bhattacharya ($G^0_N = 9 \times 10^4$ Pa).[8]

A comparison between the linear viscoelastic behavior of pure PLA and PLA stabilized with 0.25 wt % TNPP is presented in Figure 5. Master curves of the complex viscosity referenced to 180 °C constructed from isothermal curves obtained at three different temperatures (160, 180, and 200 °C) are presented. While time−temperature superposition appears to be roughly obeyed for both samples, this is not the case. The detail shown in the inset of the graph reveals that superposition is

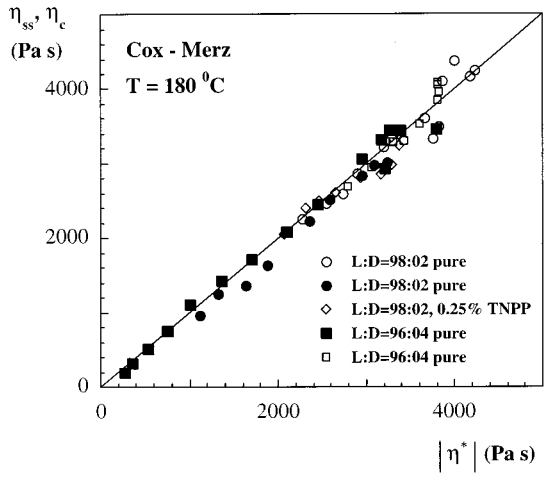

Figure 6. Comparison between dynamic $|\eta^*|$ viscosity vs reduced frequency $a_T\omega$ and the steady-state viscosity η_{ss} vs the shear rate $\dot{\gamma}$ (s^{-1}) measured in either a cone and plate (open symbols) or capillary (filled symbols) geometry. Data are for a PLA having a 98:02 ratio of L:D and a $M_w = 120\,000$ g/mol; both unstabilized (pure) and stabilized samples. Data are also shown for an unstabilized PLA having a 96:04 ratio of L:D and a $M_w = 110\,000$ g/mol. Both materials were measured at 180 °C. The Cox−Merz rule is obeyed throughout the accessible shear rates.

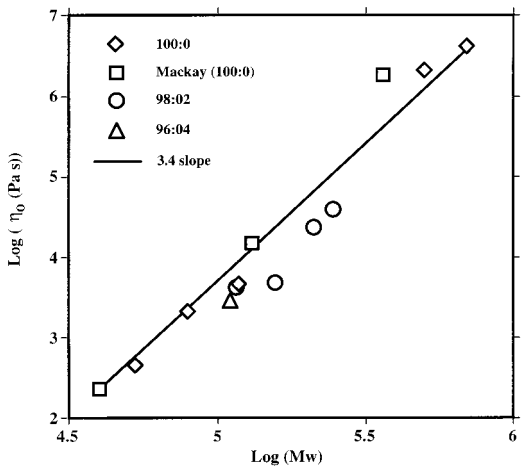

Figure 7. Scaling of the zero shear viscosity vs molecular weight. Linear regression provides a slope of 3.6; the usual 3.4 power is drawn for comparison.

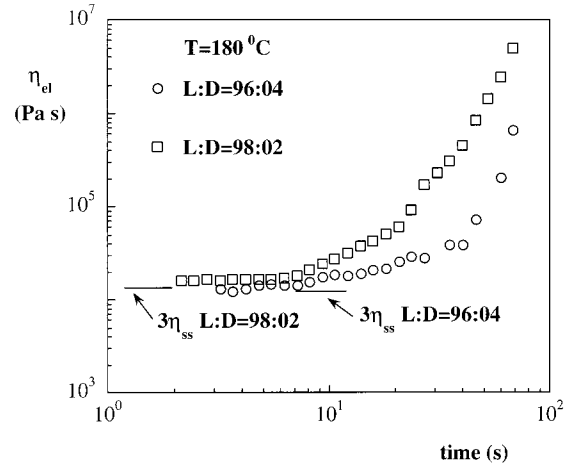

Figure 8. Growth of the elongational viscosity vs time measured at a rate of $\dot{\epsilon} = 0.1$ s^{-1}. Samples are unstabilized PLAs (nominal L:D values of 98:02 and 96:04 and corresponding weight-averaged molecular weights of 120 000 and 110 000 g/mol). Significant strain hardening is observed for Hencky strains greater than 6 (corresponding to $t > 30$ s).

not obeyed for the unstabilized sample, the scatter in data being incompatible with a master curve. However, the stabilized sample shows excellent superposition within the temperature window explored, demonstrating that the use of TNPP as a stabilizer does lead to a thermorheologically simple material response.

The Cox−Merz rule stating the equivalence of dynamic and steady shear viscosities is confirmed in Figure 6, which shows that a plot of the steady values vs the dynamic values produces a slope of unity. The results presented are for a PLAs having nominal L:D values of both 98:02 and 96:04 and corresponding to weight-averaged molecular weights of 120 000 and 110 000 g/mol, respectively. Steady shear data for these samples at low shear rates (between 0.01 and 15 s^{-1}) were collected by performing experiments in cone and plate geometry at 180 °C. It is not possible to obtain data in the cone and plate geometry for $\dot{\gamma} > 15$ s^{-1} because of the occurrence of strong flow instabilities that lead to edge fracture in the samples. Accordingly, higher shear rates were obtained from capillary measurements. Figure 6 exhibits good overall agreement between the two types of measurements throughout the shear thinning region. Usually it is found that the dynamic viscosity falls below the steady shear viscosity in the shear thinning region.[11] Whether the present agreement is due to the relatively low viscosity of PLAs or to some particular molecular feature remains an open issue. The data are slightly dispersed for high viscosity (i.e., low frequency/shear rates) due to low torques and possible degradation. The molecular weight of the PLA decreases as a result of the thermal exposure in the Haake mixer used for the addition of TNPP. Accordingly, the viscosity values of the stabilized samples consistently measure below the viscosity values of the unstabilized materials.

Scaling of viscosity with molecular weight is one of the long-standing issues in polymer rheology and is addressed in Figure 7. Several sources have been used to collect the data shown in this figure which is a plot of the logarithm of the zero shear viscosity, η_0, against the logarithm of molecular weight. Values for the PLAs discussed above are given along with data from other recent reports.[6,7] Linear regression of the data yields a slope of 3.6; the usual 3.4 power found for many polymer systems is drawn for comparison. Previous studies report much stronger scaling exponents based on more limited data sets.[6,7] It is also interesting to note that the samples measured suggest that materials containing even a few percent D-content have lower zero shear viscosities than those containing no D-stereocenters (i.e., the 100:0 samples).

Material response to extensional deformations is of particular interest in many important flows. Figure 8 presents extensional data for the same PLAs examined above (nominal L:D values of 98:02 and 96:04 and corresponding weight-averaged molecular weights of 120 000 and 110 000 g/mol). The most striking feature of the response is a strong strain hardening (the extensional viscosity increases by 2 orders of magnitude). The literature suggests that extension thickening is exhibited when the rate of deformation considerably exceeds the rate of molecular relaxation (i.e., when $\lambda_{longest} > 1/\dot{\epsilon}$).[12] This effect is normally most significant when long chain branching is present because such branching introduces very long relaxation times. How-

ever, a distinction to be noted for PLA is its extensibility; Hencky strains in excess of 10 were reached in these experiments. This ability to draw samples to large deformations without breaking is unusual for a linear polymer. Extensional behavior is explored in more detail in the modeling section of the paper given below.

Comparing the extensional viscosity growth function to the corresponding steady shear viscosity value provides a check on the validity of the data because the extensional viscosity should be 3 times the shear viscosity in the limit of low deformations. A comparison of the early time plateau value with the corresponding shear viscosity measured at $\dot{\gamma} = 0.1\ s^{-1}$ multiplied by 3 shows a reasonable agreement, the difference being only 0.5% for the 96:04 sample but about 25% in the case of the 98:02 material (see Figure 8). This later discrepancy is not surprising given the difficulties associated with extensional measurements.[9] Because the RME transducer provides limited sensitivity for measuring low forces, it is not possible to obtain the elongational data for times less than about 2 s. The agreement between extensional and shear measurements provides assurance that the extensional viscosity measurements are valid and that the observed strain hardening is a real effect.

To better understand the rheological response of PLA and to assess the ability to predict nonlinear response based on linear measurements, modeling the response to deformation using a truncated K−BKZ constitutive equation is undertaken. This equation has the form

$$\tau(t) = \int_{-\infty}^{t} m(t-t')\, h(I_1,I_2)\, \mathbf{C}^{-1}(t,t')\, dt' \qquad (1)$$

where $\tau(t)$ is the stress tensor, $m(t)$ is the memory function, $\mathbf{C}^{-1}$ is the Finger tensor, and h is the damping function. Here I_1 and I_2 stand for the first and second invariants of the Finger tensor and depend on the specifics of the flow studied. This constitutive equation has been found in the past to accurately fit both shear and extensional data.[11−14]

Several forms have been proposed in the literature for the damping function. Exponential functions have often been used.[13] In the present case, accurate prediction of shear results could not be generated without the use of a varying parameter sets. As a result, the form suggested by Papanastasiou et al. is adopted.[14] For simple shearing deformations this is

$$h(I_1,I_2) = \frac{\alpha}{\alpha + \gamma^2} \qquad (2)$$

where α is a fitting parameter. In this work, the value α = 3.66 suggested by the Doi−Edwards theory is adopted.[15] Hence, α is determined not from experimental data but from theoretical considerations.

The pure PLA data can be used to exemplify the applicability of eq 1. The memory function is given by

$$m(t) = \sum_k \frac{G_k}{\lambda_k} \exp(-t/\lambda_k) \qquad (3)$$

where the relaxation times, λ_k, and moduli, G_k, define the relaxation spectrum of the material. This spectrum may be calculated from G' and G'' data using standard nonlinear regression methods. The numerical procedure proposed by Winter and co-workers and available as the IRIS commercial software has been used.[16] The numerical values of the discrete relaxation spectrum parameters are given in parts a and b of Table 2 for both the 96:04 and 98:02 PLAs.

Table 2. Relaxation Spectrum (G_k, λ_k) Obtained from Linear Viscoelastic Data for PLA Having a Nominal L:D Ratio of 96:04 and 98:02 (for Details See Text)

G_k, Pa	λ_k, s
(a) L:D Ratio of 96:04	
3.47×10^5	1.16×10^{-3}
1.32×10^5	1.01×10^{-2}
2.64×10^4	6.37×10^{-2}
1.29×10^3	4.75×10^{-1}
(b) L:D Ratio of 98:02	
2.85×10^5	3.31×10^{-3}
4.26×10^4	3.40×10^{-2}
5.76×10^3	2.25×10^{-1}
3.19×10^2	1.47×10^{0}

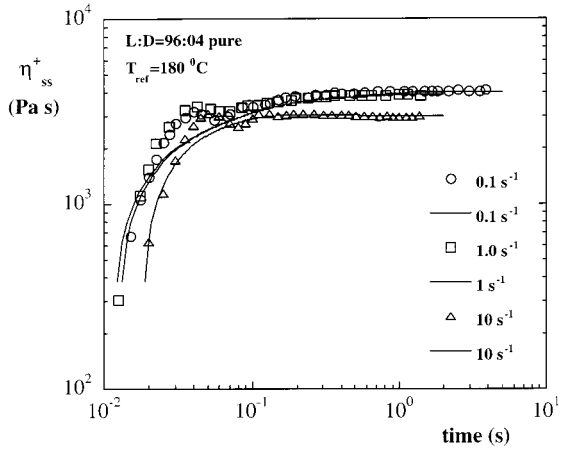

Figure 9. Comparison between the prediction of eq 4 based on linear dynamic measurements (solid lines) and the observed nonlinear response during the start-up of steady shear (open symbols). Data are for PLA having an L:D ratio of 96:04 measured for three different shear rates at $T = 180$ °C.

A priori predictions for the case of start-up of simple shear can be made using the above equations. Combination of eqs 1−3 leads to[12]

$$\eta^+(t) = tG(t)\left(\frac{\alpha}{\alpha + (\dot{\gamma}t)^2}\right) + \int_0^t sm(s)\left(\frac{\alpha}{\alpha + (\dot{\gamma}s)^2}\right) ds \qquad (4)$$

where the stress relaxation function is given by $G(t) = \sum_k G_k \exp(-t/\lambda_k)$. Comparison between predictions of eq 4 and experimental data for the 96:04 PLA chosen as an example is given in Figure 9.

A few remarks can be made regarding the results presented in Figure 9. First, for times between 0.05 and 0.1 s there is an obvious discrepancy between the experimental data and the model predictions. This is related to an experimental artifact; namely, a local peak is generated by the elasticity of the driving system and possibly the transducer of the rheometer. That is, an elastic torsion wave is generated by the instrument at short times. Despite these shortcomings, the model does capture the correct values for the steady-state viscosities at all shear rates tested for both 96:04 and 98:02 materials.

The situation for extensional deformation is much less satisfactory. Figure 10 shows the theoretical predictions for the extensional viscosity based on eq 5 which may

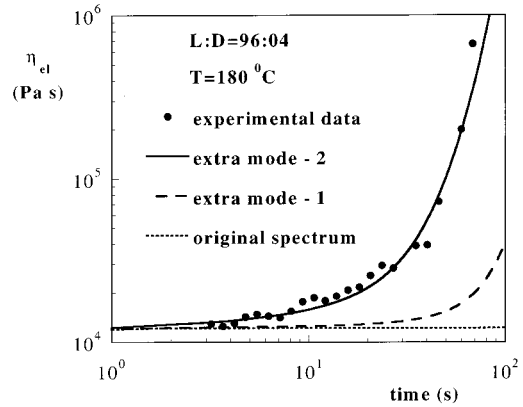

Figure 10. Comparison between experimental data measured at $\dot{\epsilon} = 0.1\ s^{-1}$ (filled symbols) and the theoretical prediction of eq 5 for the extensional viscosity based on the same dynamic spectrum values used to predict the shear viscosities shown in Figure 9 (the "original spectrum" fit), by adding a weak contribution extra mode (G_k, λ_k) = (10.1 Pa, 20 s) (the "extra mode-1" fit) and by adding a strong contribution extra mode (G_k, λ_k) = (100.1 Pa, 50 s) (the extra mode-2). The addition of a long relaxation time is required to describe the observed strain hardening.

be derived from eq 1,

$$\eta_{el}^{+}(t) = \frac{\alpha}{\dot{\epsilon}}\left[\frac{(e^{2\dot{\epsilon}t} - e^{-\dot{\epsilon}t})G(t)}{(\alpha - 3) + (2e^{\dot{\epsilon}t} + e^{-2\dot{\epsilon}t})} + \int_0^t \frac{(e^{2\dot{\epsilon}s} - e^{-\dot{\epsilon}s})m(s)}{(\alpha - 3) + (2e^{\dot{\epsilon}s} + e^{-2\dot{\epsilon}s})}\,ds\right] \quad (5)$$

where $\dot{\epsilon}$ is the constant extensional rate. One set of results (the curve fit termed "original spectrum") in Figure 10 was generated using the same linear viscoelastic spectrum parameters derived from the dynamic data (i.e., the four Maxwell modes given in Table 2a). It can be seen that no strain hardening is predicted over the experimentally studied time regimes. According to Kasehagen and Macosko, the existence of long relaxation times gives rise to strain hardening.[12] Following these authors, an attempt to predict such behavior with minimum modification of the dynamic spectrum was undertaken; a single extra relaxation mode was added to the dynamic spectrum. The mode strength was chosen to increase the zero shear viscosity by only 5% ($\lambda_k = 20.0$ s and $G_k = 10.1$ Pa). Under these conditions, strain hardening is observed within the time frame of the experiment; however, the model predictions still underestimate the extent of strain hardening (the curve fit termed "extra mode − 1"). We remark here that the relaxation time of the additional mode is much longer than the longest relaxation time $\lambda_{longest}$ obtained from the spectrum parameters, i.e.,

$$\lambda_{longest} = \frac{\sum_k G_k \lambda_k^{\,2}}{\sum_k G_k \lambda_k} = 0.1025(s) \quad (6)$$

The above value is in excellent agreement with the experimental value obtained from the G' and G'' data in the terminal region. Specifically, given the (constant) measured value of 2.5×10^{-5} Pa^{-1} for the steady-state creep compliance J_e^0 defined as

$$J_e^0 = \lim_{\omega \to 0} \frac{G'(\omega)}{G'(\omega)^2 + G''(\omega)^2} \quad (7)$$

and the zero shear viscosity $\eta_0 = 4040$ Pa·s we obtain $\lambda_{longest} = \eta_0 J_e^0 = 0.1$ s. We point out that the use of an extra mode with shorter relaxation times, i.e., $\lambda_k < 20$ s, and a corresponding higher strength G_k such that $G_k\lambda_k = 202$ Pa·s will produce even lower amounts of strain hardening.

The curve fit termed "extra mode − 2" does fit the amount of strain hardening experimentally measured. However, to obtain this fit an extra mode ($\lambda_k = 50.0$ s and $G_k = 100.1$ Pa) was added which produces, by itself, a contribution to the η_0 of the same order of magnitude as η_0 itself, which finally proves the inability of the model to account for the strong strain hardening measured.

Strain hardening for linear polymers is unusual but not unreported.[17] Of particular relevance to the present findings is a study by Koyama et al.[18] in which strain hardening is observed for linear polystyrene and poly(methyl methacrylate) upon the addition of 2 wt % ultrahigh molecular weight material. Also, Takahashi et al.[19] have reported strain hardening in linear polydisperse polystyrene and polypropylene. As can be seen from Table 1, the M_{z+1} values indicate that a high molecular weight fraction is present in the PLA samples. This high molecular weight tail is probably responsible for the observed strain hardening. The spectrum derived from the dynamic measurements is most likely incomplete because of the inability to reach very low frequencies in the experiments (this is precluded because of degradation at either long times or high temperatures). While a terminal regime is reached (as evidenced by the slopes of 2 and 1 in the G' and G'' values), this corresponds only to the longest relaxation of the majority of the chains of average molecular weight. It is known that polydispersity in bicomponent mixtures will lead to a low-frequency transition and a secondary terminal regime having slopes of 2 and 1 in the G'/G'' spectrum corresponding to the higher molecular weight component.[20−23] The existence of a high molecular weight fraction is supported by both the GPC measurements and the observation of strain hardening in extension. However, for the model used here, it is obvious that even if the full relaxation spectrum would be available, the additional mode(s) contributions would not account for the strain hardening amount experimentally observed.

There are other less likely explanations for the observed strain hardening. The stereoregularity of high L-content PLAs may allow them to form a range of structures when stretched. Helical conformations may form in the melt as a precursor to strain-induced crystallization. Such crystallization during the experiment is a possibility; however, the samples remained completely transparent, and DSC showed no evidence of an enhanced degree of crystallinity compared to samples that were cooled without having been stretched.

Conclusions

This paper present a comprehensive study on the melt rheological properties of poly(lactic acids) of high L-content (nominally greater than 96%). The most significant findings are that these materials exhibit strain

hardening in extension and that the Cox−Merz rule is obeyed far into the shear thinning region. Additionally, data from various sources are collected to show that the scaling of the zero shear viscosity is not significantly different from the usual 3.4 power and is certainly less than previously reported values that were based on fewer data. The present study concurs with previous studies in finding that the plateau modulus value for L:D = 100:0 PLA is approximately 5×10^5 Pa; this value corresponds to an entanglement molecular weight of approximately 9000 g/mol. In addition, the use of tris(nonylphenyl)phosphite (TNPP) to stabilize PLA in the melt is demonstrated. It is shown that both viscoelastic properties and weight-averaged molecular weight remain constant for extended periods of time when TNPP is added to PLA in an appropriate concentration.

There are two unique rheological features of the semicommercially produced PLAs of this study. These materials may be drawn to large Hencky strains without breaking, and they exhibit considerable strain hardening. The origin of the strain hardening appears to be a high molecular weight tail present in materials. Such a combination of rheological properties should prove advantageous for processing operations like fiber spinning, film casting, and film blowing.

An attempt based on a widely used constitutive law, i.e., a truncated K−BKZ equation, to model the strain hardening does not produce the adequate fit even if an extra mode—whose contribution to the η_0 is about 5%—is added. The model does correctly fit the extensional data only if a mode whose contribution is of the same order as the η_0 is added, which is physically unacceptable. Therefore, it is necessary to formulate a more adequate constitutive equation, and this will be reported in a subsequent paper.

Acknowledgment. The present study has been aided by numerous individuals. Dr. David Giles and Professor Christopher Macosko were instrumental in providing access to the RME at the University of Minnesota. Dr. Cora Leibig of the Dow Chemical Company and Professor Michael Mackay of the Stevens Institute of Technology provided data that appears in Figure 7. The PLA samples for this study were provided by Kevin McCarthy and Dr. Michael Mang of the Cargill-Dow Polymers Co. The majority of support for this study was provided by a grant from the EPA Technologies for Sustainable Environment Program (R 826733-01-0). Additional assistance was provided by an NSF CAREER Award to John Dorgan (CTS-950246). The sponsorship of these agencies is gratefully acknowledged.

References and Notes

(1) Dorgan, J. R. *Poly(lactic acid) Properties and Prospects of an Environmentally Benign Plastic*; American Chemical Society: Washington, DC, 1999; pp 145−149.
(2) Cargill-Dow Polymers, Environmental Benefits and Disposal Options, available at www.cdpoly.com.
(3) Cornelis, A. P.; Joziasse, H. V.; Grijpma, D. W. *Macromol. Chem. Phys.* **1996**, *197*, 2219−2229.
(4) Grijpma, D. W.; Penning, J. P.; Pennings, A. J. *Colloid Polym. Sci.* **1994**, *272*, 1068−1081.
(5) Witzke, D. R. Introduction to Properties, Engineering, and Prospects of Polylactide Polymers. Ph.D. Thesis, Michigan State University, 1997.
(6) Cooper-White, J. J.; Mackay, M. M. *J. Polym. Sci., Part B: Polym. Phys.* **1999**, *37*, 1803−1812.
(7) Dorgan, J. R.; Williams, J. S.; Lewis, D. N. *J. Rheol.* **1999**, *43*, 1141−1155.
(8) Ramkumar, D. H. S.; Bhattacharya, M. *Polym. Eng. Sci.* **1998**, *38*, 1426−1435.
(9) Schulze, J. S.; Lodge, T. P.; Macosko, C. W. *J. Rheol.*, in press.
(10) Cheung, M. F.; Carduner, K. R.; Golovoy, A.; Van Oene, H. *J. Appl. Polym. Sci.* **1990**, *40*, 977−987.
(11) Dealy, J. M.; Wissbrun, K. F. *Melt Rheology and Its Role in Plastics Processing*; Van Nostrand Reinhold: New York, 1990.
(12) Kasehagen, L. J.; Macosko, C. W. *J. Rheol.* **1998**, *42*, 1303−1327.
(13) Wagner, M. H. *J. Non-Newtonian Fluid Mech.* **1976**, *4*, 39−55.
(14) Papanastasiou, A. C.; Scriven, L. E.; Macosko, C. W. *J. Rheol.* **1983**, *24*, 847−867.
(15) Doi, M.; Edwards, S. F. *The Theory of Polymer Dynamics*; Oxford University Press: New York, 1986.
(16) Baumgaertel, M.; DeRosa, M. E.; Machado, J.; Masse, M.; Winter, H. H. *Rheol. Acta* **1992**, *31*, 75.
(17) Münstedt, H.; Laun, H. M. *Rheol. Acta* **1981**, *20*, 211−221.
(18) Koyama, K.; Takahashi, T.; Naka, Y.; Takimoto, J. Preprints of the Polymer Processing Society International Meeting, MS. No. PPS-13 8B, 1997.
(19) Takahashi, M.; Isaki, T.; Takigawa, T.; Masuda, T. *J. Rheol.* **1993**, *37*, 827−846.
(20) Struglinski, M. J.; Graessley, W. W.; Fetters, L. J. *Macromolecules* **1988**, *21*, 783−790.
(21) Berger, L.; Meissner, J. *Rheol. Acta* **1992**, *31*, 63−74.
(22) Palade, L. I.; Verney, V.; Attané, P. *Macromolecules* **1995**, *28*, 7051−7057.
(23) Palade, L. I.; Verney, V.; Attané, P. *Rheol. Acta* **1996**, *35*, 265−273.

MA001173B